Received: 22 February 2021 | Accepted: 14 June 2021

DOI: 10.1111/2041-210X.13682

RESEARCH ARTICLE

Methods in Ecology and Evolution BRITISH ECOLOGICAL SOCIETY

Measuring temporal change in alpha diversity: A framework integrating taxonomic, phylogenetic and functional diversity and the iNEXT.3D standardization

Anne Chao[1] | Peter A. Henderson[2] | Chun-Huo Chiu[3] | Faye Moyes[4] | Kai-Hsiang Hu[1] | Maria Dornelas[4] | Anne E. Magurran[4]

[1]Institute of Statistics, National Tsing Hua University, Hsin-Chu, Taiwan

[2]Pisces Conservation, IRC House, The Square, Pennington, Lymington, UK

[3]Department of Agronomy, National Taiwan University, Taipei, Taiwan

[4]Centre for Biological Diversity and Scottish Oceans Institute, School of Biology, University of St Andrews, St Andrews, Fife, UK

Correspondence
Anne Chao
Email: chao@stat.nthu.edu.tw

Funding information
Taiwan Ministry of Science and Technology, Grant/Award Number: NERC-MOST 108-2923-M-007-003; Natural Environment Research Council, UK, Grant/Award Number: NE/T004487/1; Leverhulme Trust, Grant/Award Number: RPG-2019-402

Handling Editor: Will Pearse

Abstract

1. Biodiversity is a multifaceted concept covering different levels of organization from genes to ecosystems. Biodiversity has at least three dimensions: (a) Taxonomic diversity (TD): a measure that is sensitive to the number and abundances of species. (b) Phylogenetic diversity (PD): a measure that incorporates not only species abundances but also species evolutionary histories. (c) Functional diversity (FD): a measure that considers not only species abundances but also species' traits.
2. We integrate the three dimensions of diversity under a unified framework of Hill numbers and their generalizations. Our TD quantifies the effective number of equally abundant species, PD quantifies the effective total branch length, mean-PD (PD divided by tree depth) quantifies the effective number of equally divergent lineages, and FD quantifies the effective number of equally distinct virtual functional groups (or functional 'species'). Thus, TD, mean-PD and FD are all in the same units of species/lineage equivalents and can be meaningfully compared.
3. Like species richness, empirical TD, PD and FD based on sampling data depend on sampling effort and sample completeness. For TD (Hill numbers), the iNEXT (interpolation and extrapolation) standardization was developed for standardizing sample size or sample completeness (as measured by sample coverage, the fraction of individuals that belong to the observed species) to make objective comparisons across studies. This paper extends the iNEXT method to the iNEXT.3D standardization to encompass all three dimensions of diversity via sample size- and sample coverage-based rarefaction and extrapolation under the unified framework. The asymptotic diversity estimates (i.e. sample size tends to infinity and sample coverage tends to unity) are also derived. In addition to individual-based abundance data, the proposed iNEXT.3D standardization is adapted to deal with incidence-based occurrence data.
4. We apply the integrative framework and the proposed iNEXT.3D standardization to measure temporal alpha-diversity changes for estuarine fish assemblage data spanning four decades. The influence of environmental drivers on diversity change are also assessed. Our analysis informs a mechanistic interpretation of

[Correction added on 27 October 2022, after first online publication: The Chao et al. (2021) reference has been split into Chao (2021) and Chao et al. (2021)].

biodiversity change in the three dimensions of diversity. The accompanying freeware, iNEXT.3D, developed during this project, facilitates all computation and graphics.

KEYWORDS
functional diversity, Hill numbers, iNEXT standardization, phylogenetic diversity, sample coverage, taxonomic diversity

1 | INTRODUCTION

Ecosystems are under escalating threat as a consequence of anthropogenic pressures on the environment. Biodiversity is clearly imperilled, but the nature of ongoing biodiversity change is complex (Daskalova et al., 2020; Frishkoff et al., 2014; Helmus et al., 2014), and not well-understood. Recent work has focused on temporal change in taxonomic alpha diversity (the numbers and relative abundances of species) of assemblages (e.g. Chase et al., 2020; Dornelas et al., 2014), but, as is increasingly becoming apparent, biodiversity is more than just taxonomic diversity. The IPBES Conceptual Framework, for instance, states that biodiversity includes 'variation in genetic, phenotypic, phylogenetic and functional attributes, as well as changes in abundance and distribution over time and space, within and among species, biological communities and ecosystems' (Díaz et al., 2015, p. 8). Disentangling changes across these different dimensions of biodiversity is essential to understand ongoing biodiversity change.

Historically, the measurement of taxonomic diversity has received the greatest attention (Magurran & McGill, 2011; Southwood & Henderson, 2000). There is, nonetheless, a rapidly growing literature on phylogenetic diversity metrics (e.g. Cadotte & Davies, 2016; Chao et al., 2010; Faith, 1992; Swenson, 2019; Tucker et al., 2017 and references therein) and in the assessment of functional diversity or trait diversity (e.g. Bjorkman et al., 2018; Cadotte et al., 2011; Chao et al., 2019; Diaz & Cabido, 1997; Petchey & Gaston, 2002; Pillar & Duarte, 2010; Tilman et al., 1997). To date, a typical approach has been to quantify each dimension (taxonomic (TD), functional (FD), phylogenetic (PD)) of diversity independently (see for example, Maire et al., 2015; Tucker et al., 2017; Villéger et al., 2017). The three different dimensions are quantified using customized metrics and analysed in isolation or compared using correlational approaches. Moreover, species abundances are not considered in some measures (e.g. species richness for TD, or total branch length for PD), whereas only highly abundant species are considered in some other measures (e.g. Rao's quadratic entropy or mean phylogenetic/functional distance for PD and FD; Arnan et al., 2017; Chun & Lee, 2017; Rao, 1982). Further insight can be gained by integrating analysis of TD, FD and PD to help us identify when patterns are consistent versus when they are different across the three axes of biodiversity.

An integrative framework of biodiversity change bringing together temporal change in these multiple dimensions of diversity and also encompassing measures with and without incorporating species abundances can expand our insights into ongoing change. This integrative approach would have the potential to explicitly relate change in one dimension of diversity to change, or stasis, in another, and to link assemblage responses to anthropogenic impacts and environmental perturbations. Yet, to achieve this, we must first express change in the different dimensions with comparable metrics. For this purpose, we propose (in Section 2) a unified framework based on Hill numbers and their generalizations. Our unified framework integrates three dimensions of diversity: the ordinary Hill numbers (Hill, 1973) for TD, the PD measures derived in Chao et al. (2010), and the FD measures developed recently by Chao et al. (2019).

To express change in comparable units, in our framework, TD quantifies the effective number of equally abundant species, PD quantifies the effective total branch length, mean-PD (PD divided by tree depth) quantifies the effective number of equally divergent lineages, and FD quantifies the effective number of equally distinct virtual functional groups (or functional 'species'). The standardization of units across the three dimensions makes comparisons meaningful. It can also take account of the fact that time is uni-directional, and involves temporal autocorrelation (Dornelas et al., 2013) to examine lagged effects and infer causal links. In most assemblages, species abundances vary widely, with a few extremely abundant species and many rare species. Therefore, metrics that ignore abundance are largely driven by the rare species, whereas metrics that use abundance are overwhelmingly tracking change in the dominant species. By using a Hill numbers approach, our framework allows tuning the effect of abundance on the diversity metrics. All the diversity measures are indexed by a diversity order $q \geq 0$, which controls the sensitivity of the measure to species abundance; thus measures with and without considering species/node abundance can be included in the same formula. Moreover, researchers can focus on rare, abundant or dominant species by varying the parameter q, and disentangle their effects on diversity change.

In practice, all biodiversity assessments are based on sampling data. Diversity measures based on sampling data depend on sampling effort and sample completeness. Observed diversity for incomplete sampling data cannot be directly compared unless sampling effects are controlled for through standardization. Throughout the paper, sample completeness is measured by sample coverage (or simply coverage), that is, the fraction of individuals that belong to

the observed species. This is a concept originally developed by Alan Turing and I. J. Good in their cryptographic analysis during World War II (Good, 1953). Focusing on TD (Hill numbers), Chao et al. (2014) proposed an iNEXT standardization on the basis of equal sample size or sample coverage. The software iNEXT (Hsieh et al., 2016) was developed to facilitate all computations and graphics. In Section 3, we extend the iNEXT method to iNEXT.3D standardization encompassing all three dimensions of diversity via size- and coverage-based rarefaction and extrapolation under our unified framework. The corresponding asymptotic diversity estimates are also derived. All R codes along with data used in this paper are archived; see Data Accessibility.

We illustrate in Section 4.1 the iNEXT.3D standardization with an analysis of an exceptionally comprehensive estuarine fish assemblage data spanning four decades (Henderson & Holmes, 1991; Henderson et al., 2011; Magurran & Henderson, 2003). In Section 4.2, we show how the framework can be used to evaluate the influence of environmental drivers on biodiversity change in each dimension of biodiversity. Ecological interpretations of our analysis are discussed in Section 5; conclusions are provided in Section 6.

2 | A UNIFIED FRAMEWORK INTEGRATING TD, PD AND FD

2.1 | Hill number of order *q*

Hill numbers (Hill, 1973) have been increasingly used to quantify species/taxonomic diversity of an assemblage. Assume that there are S species in an assemblage, indexed by $i = 1, 2, \ldots, S$. Let z_i represent the raw abundance (number of individuals) of species i, or other metrics of species dominance, such as biomass, coverage of corals or basal area of plants. The total abundance in the assemblage is expressed as $z_+ = \sum_{i=1}^{S} z_i$. Here $p_i = z_i/z_+$ denotes the *relative* abundance of the individuals of species i in the assemblage, $\sum_{i=1}^{S} p_i = 1$.

Hill number or TD of order q is defined as the following function in terms of species relative abundances:

$$ {}^{q}TD = \left(\sum_{i=1}^{S} \left(\frac{z_i}{z_+} \right)^{q} \right)^{1/(1-q)} = \left(\sum_{i=1}^{S} p_i^{q} \right)^{1/(1-q)}, \quad q \geq 0, \quad q \neq 1, \quad (1) $$

which is interpreted as the effective number of species. The parameter q determines the sensitivity of the measure to the relative abundance of species. To assess diversity change, we focus on the Hill numbers of $q = 0$, 1 and 2, which unify three well-established indices of biodiversity: (a) TD of $q = 0$ reduces to species richness. (b) TD of $q = 1$ reduces to Shannon diversity (the exponential of Shannon entropy), which can be be interpreted as the effective number of common or abundant species. (c) TD of $q = 2$ reduces to Simpson diversity (the inverse of the Simpson concentration index), which can be be interpreted as the effective number of dominant or highly abundant species; see Appendix S1 for details.

2.2 | A unified framework: The attribute diversity or Hill-Chao numbers

As indicated in Section 1, biodiversity includes 'variation in genetic, phenotypic, phylogenetic, and functional attributes.' Here we propose a unified *attribute-diversity* approach that integrates ordinary Hill numbers for TD, the PD measures derived in Chao et al. (2010), and the FD measures developed by Chao et al. (2019). In this context, a *taxonomic attribute* means a species in TD, a *phylogenetic attribute* means a unit-length branch segment in a phylogenetic tree in PD, and a *functional attribute* means a virtual functional group in FD. In the unified framework, all measures can be formulated as Hill numbers of a *hypothetical* assemblage which is decomposed into M sub-assemblages: the i-th sub-assemblage consists of v_i attributes, each with raw abundance a_i, $i = 1, 2, \ldots, M$. The total abundance among all attributes is denoted as $V = \sum_{i=1}^{M} v_i a_i$. Thus, the relative abundance of any attribute in the i-th sub-assemblage is a_i/V. The *attribute diversity* (AD) or *Hill-Chao numbers* of order q is defined as the Hill number of order q for the hypothetical assemblage:

$$ {}^{q}AD = \left(\sum_{i=1}^{M} v_i \left(\frac{a_i}{\sum_{j=1}^{M} v_j a_j} \right)^{q} \right)^{1/(1-q)} = \left(\sum_{i=1}^{M} v_i \left(\frac{a_i}{V} \right)^{q} \right)^{1/(1-q)} \quad q \geq 0, \quad q \neq 1. \quad (2) $$

See Table 1 for the AD formulas of $q = 0$, 1 and 2. For $q = 0$, AD is interpreted as the total effective number of attributes (i.e. attribute richness). For $q = 1$ and $q = 2$, AD can be interpreted, respectively, as the effective number of abundant and dominant attributes. Table 1 also summarizes the formulas of TD, PD and FD and their corresponding values of M, v_i and abundance a_i, $i = 1, 2, \ldots, M$, as special cases of Hill-Chao numbers. Some details are described below.

2.2.1 | TD as a special case of Hill-Chao numbers

For TD, each sub-assemblage comprises of only one species. That is, letting $M = S$, $v_i = 1$ and $a_i = z_i$ (raw abundance of species i) for $i = 1, 2, \ldots, S$, we have total abundance $V = z_+$, and $a_i/V = p_i$ (relative abundance of species i). Then Equation (2) reduces to the ordinary Hill number of order q.

2.2.2 | PD as a special case of Hill-Chao numbers

Assume that all species of an assemblage are connected by a rooted ultrametric phylogenetic tree, with the S species as tip nodes. Chao et al. (2010) pointed out that one must specify the time period that PD refers to. They introduced an additional parameter T (time reference point) for quantifying PD. In our applications, the reference time is chosen to be the age of the root of the phylogenetic tree spanned by all species in the assemblage.

Within the phylogenetic tree with depth T, assume that there are B branches/nodes. Let L_i denote the length of the i-th branch. For $i = 1, 2, \ldots, B$, define z_i^* (and p_i^*) as the total absolute (and relative)

abundance descended from the *i*-th branch/node. A widely used measure is the total branch length (Faith's PD) in the phylogenetic tree (Faith, 1992), but species/node abundance is disregarded. Chao et al. (2010) extended Faith's PD to incorporate species/node abundances. Their approach can be fit into the unified framework by treating each unit-length branch segment as a phylogenetic attribute. That is, they considered a *hypothetical* assemblage which can be decomposed into B sub-assemblages: the i-th sub-assemblage consists of L_i attributes (unit-length branch segments) each with node abundance z_i^*. In other words, letting $M = B$, $v_i = L_i$ and $a_i = z_i^*$ (abundance of node i) in Equation (2) for $i = 1, 2, \ldots, B$, we have $V = z_+T$, and $a_i/V = p_i^*/T$. Equation (2) then reduces to the ${}^qPD$ measure derived in Chao et al. (2010, their eq. 4.4); see Table 1 for formulas.

The ${}^qPD$ measure is interpreted as the effective total phylogenetic attributes or effective total branch length (because each phylogenetic attribute is unit-length). Dividing ${}^qPD$ by tree depth, we obtain the *mean* ${}^qPD$ (mean-PD of order q) measure derived by Chao et al. (2010, their eq. 4.5). This measure quantifies the effective number of equally abundant and equally divergent species/lineages, each with lineage length T. Thus, mean-PD has the same units as TD. When there are no interior nodes in the phylogenetic tree, *mean* ${}^qPD$ reduces to TD of order q. The mean-PD measures of the three orders $q = 0$, 1 and 2 unify three previous PD indices: mean-PD of $q = 0$ reduces to Faith's PD divided by tree depth; mean-PD of $q = 1$ and $q = 2$ are, respectively, simple transformations of phylogenetic entropy and Rao's quadratic entropy; see Appendix S1 for details.

2.2.3 | FD as a special case of Hill-Chao numbers

When each of the species is characterized by one or more traits, a wide range of approaches have been proposed to quantify FD; see Chao et al. (2019) for a review. Our framework is based on species pairwise distances computed from the Gower distance (Gower, 1971), which can deal with both categorical traits and continuous traits.

Chao et al. (2019) introduced to FD an essential parameter: τ (tau)—the threshold of functional distinctiveness between any two species; τ can be chosen to be *any* positive value. Any two species with functional distance $\geq \tau$ are treated as functionally equally distinct at the threshold level of τ. The idea was motivated by statistical clustering: imagine that all species are placed in a functional space with specified pairwise distances, and they are classified into virtual functional groups. As in most clustering algorithms, one must first determine a threshold level such that any two species with distance greater than or equal to the specified threshold level are in different clusters and vice versa. If the threshold is set to be very low, then each species forms a functional group and all species are equally distinct from each other. This reduces to TD. By contrast, if we use a very high threshold, then nearly all species are classified into a single group (i.e. FD tends to 1) and thus the diversity measure becomes weakly sensitive to species abundances and traits.

Since two or more species may be functionally similar to some extent, or even functionally identical, Chao et al. (2019) first expand the set of individuals belonging to species i to *a functionally indistinct* set of species i, for any specified level τ. The abundance of the functionally indistinct set of species i is denoted as $a_i(\tau)$; see Table 1 for formulas. When the 'abundance' of species i is expanded to $a_i(\tau)$, the contribution of species i after its functional redundancy with other species is accounted for is reduced to a proportion $v_i(\tau) = z_i/a_i(\tau)$ of the group, so each individual is only counted once in the formulation.

Chao et al.'s (2019) approach can be fit into the unified framework by treating each virtual functional group as a functional attribute. They considered a *hypothetical* assemblage which is decomposed into S sub-assemblages with the i-th sub-assemblage consisting of $v_i(\tau) = z_i/a_i(\tau)$ functional attributes, each with abundance $a_i(\tau)$, $i = 1, 2, \ldots, S$. That is, letting $M = S$, $v_i = v_i(\tau)$, and $a_i = a_i(\tau)$ in Equation (2), for $i = 1, 2, \ldots, S$, we have $V = z_+$, and $a_i/V = a_i(\tau)/z_+$. Equation (2) then reduces to the ${}^qFD$ measure derived in Chao et al. (2019, their eq. 4); see Table 1 for formulas. The measure ${}^qFD$ quantifies the effective number of equally distinct functional groups (or functional 'species') at a given threshold level τ. FD of order $q = 0$ reduces to the total effective number of functional groups (functional-group richness) at a given threshold τ. FD of $q = 1$ and $q = 2$ are, respectively, simple transformations of Shannon-entropy-type index and Rao's quadratic entropy; see Appendix S1 for details.

When the threshold level τ is low (specifically, τ is less than the minimum of all non-zero pairwise distances), we have $a_i(\tau) = z_i$ and $v_i(\tau) = 1$; each species forms a functional group and ${}^qFD$ reduces to TD of order q. When the threshold level τ is very high, we have $a_i(\tau) = z_+$ and $v_i(\tau) = z_i/z_+$; all species forms a functional group and ${}^qFD$ approaches to 1 for all orders q. FD generally declines with increasing threshold level; see figure 1 of Chao et al. (2019) for an example. Since Gower distance is between 0 and 1, we can consider *all plausible thresholds* in the interval [0, 1] and depict ${}^qFD$ as a decreasing function of τ. In our applications, we compute the area under the τ-profile in [0, 1] and obtain an overall, integrated functional measure, which is referred to as AUC (area under the curve of a τ-profile).

3 | THE iNEXT.3D STANDARDIZATION

As indicated in the Introduction, the observed TD, PD and FD values based on incomplete survey data depend on sampling effort and sample completeness. A statistical solution to remove this dependence is to infer the asymptotic or true diversity of entire assemblages. Nevertheless, sufficient data are required to accurately infer the true diversity, otherwise the asymptotic estimates obtained from incomplete data may be subject to bias. Typical biodiversity data are sufficient to accurately estimate diversity measures of $q = 1$ and 2 because abundant/dominant species would be observed in any sample. When data are not sufficient to infer the entire assemblage (especially for measures of $q = 0$), Chao et al. (2014) proposed the non-asymptotic iNEXT standardization via size- and coverage-based rarefaction and extrapolation to compare TD across multiple

TABLE 1 Taxonomic, phylogenetic and functional diversities are integrated under a unified framework based on attribute diversity (Hill-Chao numbers). TD, PD and FD of $q = 0$, 1 and 2 can be obtained by substituting the appropriate v_i and a_i values listed in the table into the AD formulas. Here an attribute means a species in TD, a unit-length branch segment in a phylogenetic tree in PD, or a virtual functional group in FD

Diversity	Number of sub-assemblages (M)	Number of attributes in the i-th sub-assemblage	Abundance of each attribute in the i-th sub-assemblage	Total abundance across all attributes	Effective number of attributes
Unified framework: Attribute diversity (AD) or Hill-Chao numbers	S or B	v_i	a_i	$V = \sum_{i=1}^{M} v_i a_i$	${}^qAD = \left(\sum_{i=1}^{M} v_i \left(\frac{a_i}{V}\right)^q\right)^{1/(1-q)}$ ${}^0AD = \sum_{i=1}^{M} v_i$ ${}^1AD = \lim_{q\to 1} {}^qAD = \exp\left(-\sum_{i=1}^{M} v_i \frac{a_i}{V}\log\frac{a_i}{V}\right)$ ${}^2AD = 1/\sum_{i=1}^{M} v_i (a_i/V)^2$
Taxonomic diversity (TD)	S (# of species)	1 (species)	z_i (abundance of species i)	$V = \sum_{i=1}^{S} z_i = z_+$ (total abundance)	${}^qTD = \left(\sum_{i=1}^{S} \left(\frac{z_i}{z_+}\right)^q\right)^{1/(1-q)}$
Phylogenetic diversity (PD)	B (# of branches/nodes) in a tree with depth T	L_i (length of branch i)	z_i^* (abundance of branch/node i)	$V = \sum_{i=1}^{B} L_i z_i^* = z_+ T$	${}^qPD = \left(\sum_{i=1}^{B} L_i \left(\frac{z_i^*}{z_+ T}\right)^q\right)^{1/(1-q)}$ $(mean\ {}^qPD = {}^qPD/T)$
Functional diversity* (FD)	S (# of species)	$v_i(\tau)$ (functional groups contributed by species i)	$a_i(\tau)$ (abundance of functionally indistinct set of species i)	$V = \sum_{i=1}^{S} v_i(\tau) a_i(\tau) = z_+$ (total abundance)	${}^qFD = \left(\sum_{i=1}^{S} v_i(\tau) \left(\frac{a_i(\tau)}{z_+}\right)^q\right)^{1/(1-q)}$

*Formulas for FD: $a_i(\tau) = z_i + \sum_{j\neq i}\left(1 - \frac{d_{ij}(\tau)}{\tau}\right) z_j = \sum_{j=1}^{S}\left(1 - \frac{d_{ij}(\tau)}{\tau}\right) z_j$, and $v_i(\tau) = z_i/a_i(\tau)$ for a specified threshold level τ. Here d_{ij} denotes the trait-based Gower distance between species i and species j; $d_{ij}(\tau) = \min(\tau, d_{ij})$.

assemblages. Hsieh and Chao (2017) extended the iNEXT method to the phylogenetic version. Here, we extend the iNEXT method to the iNEXT.3D standardization for three dimensions of diversity. Derivation details are provided in Appendix S2 with a summary table of formulas (Table S2.1).

At the data level, assume an empirical sample of n individuals is taken from a focal assemblage. We call this observed sample (including species abundances, species traits and the observed phylogenetic tree) the *reference* sample. Let X_i denote the sample abundance/frequency of the i-th species in the reference sample; only species with $X_i > 0$ are observed, $\sum_i X_i = n$. In statistical inferences based on sampling data, all assemblage-level variables in Table 1 are replaced by observed data in the reference sample.

Under the unified framework presented in Section 2.2, let ${}^qAD(m)$ be the expected attribute diversity (Hill-Chao numbers) that would be observed in a hypothetical sample of size $m \geq 1$. Let $C(m)$ be the expected sample coverage. Chao and Jost (2012) derived an interpolated coverage estimator $\widehat{C}(m)$ for any rarefied sample of size $m < n$, and an extrapolated coverage estimator $\widehat{C}(n+m^*)$ for any augmented sample of size $n + m^*$. In the iNEXT.3D standardization (Appendix S2), we derive the corresponding rarefied estimators ${}^q\widehat{AD}(m)$ and extrapolated estimator ${}^q\widehat{AD}(n+m^*)$ with bootstrapped confidence intervals. Then the following two types of rarefaction and extrapolation sampling curves under the unified framework can be obtained.

3.1 | Sample size-based rarefaction/extrapolation curve for Hill-Chao numbers

The proposed size-based sampling curve for ${}^qAD$ includes the rarefaction part (which plots ${}^q\widehat{AD}(m)$ as a function of m, where $m < n$) and the extrapolation part (which plots ${}^q\widehat{AD}(n+m^*)$ as a function of $n + m^*, m^* > 0$). The two parts join smoothly at the point of the reference sample, and the confidence intervals based on the bootstrap method also join smoothly. For the measure $q = 0$, the size can be extrapolated, at most, to no more than double the reference sample size (Chao et al., 2014). For the measures with $q = 1$ and $q = 2$, if data are not sparse, the extrapolation can be reliably extended to infinity to attain the estimated asymptotes.

The size-based standardization represents the traditional approach in ecology. However, the diversity estimates for samples with a standardized size do not satisfy an essential requirement for diversity (i.e. replication principle). Thus the magnitude of the difference in diversity among assemblages is much compressed (Chao & Jost, 2012, their table 1). In contrast, coverage-based standardization (see below) to a given degree of sample coverage satisfies the replication principle. We thus only focus on the coverage-based rarefaction and extrapolation in our later applications. Nevertheless, this type of size-based sampling curve can be used to visually determine whether data are sufficient to provide reliable asymptotic diversity estimates (Chao et al., 2020), as will be illustrated in our data analysis (Section 4.1).

3.2 | Coverage-based rarefaction/extrapolation curve for Hill-Chao numbers

Our proposed coverage-based sampling curve for ${}^qAD$ includes rarefaction (which plots ${}^q\widehat{AD}(m)$ with respect to $\widehat{C}(m)$) and extrapolation (which plots ${}^q\widehat{AD}(n+m^*)$ with respect to $\widehat{C}(n+m^*)$) joining smoothly at the reference sample point. The confidence intervals based on the bootstrap method also join smoothly. For the measure $q = 0$, the extrapolation can be extended to the coverage corresponding to double the reference sample size. For the measures with $q = 1$ and $q = 2$, if data are not sparse, the extrapolation can often be extended to the coverage of unity to attain the estimated asymptotes.

When comparing many assemblages, as in the case of our applications, we only restrict our comparison to two standardized coverage values (Chao et al., 2020).

1. C_{min}: first compute the observed sample coverage for each sample; C_{min} is the minimum among all observed coverage values. Then all samples are *rarefied* to C_{min}. Since only rarefaction is involved, the diversity estimates are nearly unbiased, but this will result in some data being thrown away.
2. C_{max}: to avoid throwing away data, each sample is first extrapolated to double the reference sample size. Then C_{max} is the minimum among the coverage values obtained from those extrapolated samples.

3.3 | Extending to incidence data

In many biodiversity surveys, recording species incidence (detection/non-detection) in multiple sampling units is more practical than enumerating individuals. For example, counting the individuals in a flock, herd or school may be difficult; it is sometimes impossible to count individuals of microbes, ants and clonal plants. In such cases, the sampling unit is often a trap, net, quadrat, plot or a fixed time period and only species' detection/non-detection records in each sampling unit are available.

Colwell et al. (2012) and Chao et al. (2014) demonstrated that replicated incidence data support statistical approaches to the biological inference that are as powerful as the corresponding abundance-data-based approaches. Most importantly, analyses based on multiple incidence data are less sensitive to clustering or aggregation of individuals, compared to those based on abundance data (Chao et al., 2020; Colwell et al., 2012). In Appendix S3, we briefly show that the iNEXT.3D standardization can be adapted to deal with replicated incidence data.

4 | APPLICATION

We applied the proposed iNEXT.3D standardization to the four-decade time series of estuarine fishes collected at Bridgwater Bay in UK's Bristol Channel from 1981 to 2019 using consistent sampling schemes;

see Henderson and Holmes (1991), Magurran and Henderson (2003) and Henderson et al. (2011) for sampling details, and see Chao (2021) and Chao et al. (2021) for data and R code. A total of 88 species were caught and their monthly abundances were recorded. The data for 1986 are excluded because sampling was not conducted for several months. All pertinent summary statistics computed from the 38 yearly datasets are tabulated in Table S4.1 in Appendix S4.

The phylogenetic tree for the 88 species is shown in Figure S4.1. The tree depth is normalized to unity, so our PD and mean-PD are identical. FD measures are based on the species-pairwise Gower distances computed from 12 traits. There are nine continuous traits (mean weight, length of first maturity, trophic level, mean temperature preference, maximum weight, growth rate, food consumption and biomass, maximum depth and generation time) and three categorical traits (position in water column, reproductive guild and body shape). Five environmental variables for each month are also available; see Section 4.2.

4.1 | Diversity analysis based on the iNEXT.3D standardization

4.1.1 | Yearly abundance data (Figures 1 and 2)

We first present the diversity analysis based on the yearly abundance data, formed by pooling the monthly abundances within each year. Table S4.1 shows that the number of species found in yearly data ranges from 32 (in 2009, 2012) to 46 (in 1998); there are singletons (species represented by only one individual) every year, signifying that sampling is incomplete and some species were undetected in yearly data (Chao et al., 2020). As a preliminary analysis, we first applied the iNEXT.3D standardization to *each* yearly data. For the abundance data of 1981, the iNEXT.3D output including the size- and coverage-based rarefaction and extrapolation sampling curves for TD, PD and FD is shown in Appendix S4 (Figures S4.2 and S4.3); the corresponding curves for other years exhibit similar patterns and thus are omitted. All size-based plots reveal that the curves for diversity measures of $q = 1$ and $q = 2$ generally level off, implying that the corresponding asymptotic estimates can be used to accurately infer the true diversities of entire assemblages. However, none of the curves for measures of $q = 0$ stabilize, even after doubling the size of the reference sample, implying that our asymptotic TD, PD and FD estimates of $q = 0$ represent only the lower bounds. Thus, fair comparison should then be based on standardized sample coverage. As discussed in Section 3, we focus on two coverage values, that is, C_{max} and C_{min}, based on 38 yearly samples.

The sample coverage for each year is very high, ranging from 99.59% (in 2019) to 99.93% (in 1998) because there were very dominant species every year. Although differences among yearly coverage values are little, a tiny fraction of the assemblage's individuals may contain many species due to the potential presence of vanishingly rare species. Figure 1 shows the temporal patterns for the four diversity estimation methods yielding diversity values from high to low: the asymptotic diversity estimates (column 1), the standardized diversity under the coverage value of C_{max} = 99.75% (column 2, extrapolation is involved), the observed diversity (column 3) and the standardized diversity under the coverage value of C_{min} = 99.59% (column 4, only rarefaction is involved). To demonstrate the relative magnitude of TD, PD and FD, the plots in Figure 2 display the three dimensions of diversity in the same figure for each fixed order $q = 0$, 1 and 2.

4.1.2 | Incidence data (Figures 3 and 4)

To avoid the effect of intra-specific aggregation and the dominance of very abundant species, we also examined the temporal diversity patterns based on incidence-based occurrence data. We treat each month as a sampling unit and extract the species incidence (detection/non-detection) in a month to obtain an occurrence count (incidence-based frequency) of each species in three consecutive years. Thus, a total of 36 time periods (1981–1983, 1982–1984, ..., 2016–2018, 2017–2019) are involved. All summary statistics are tabulated in Table S4.2.

We applied the same analyses for yearly abundance data to the 3-year incidence-based data. The number of species found in each 3-year period ranges from 45 (in 2009–2011) to 59 (in 1998–2000). Table S4.2 shows that there were species that were caught in only 1 month in each 3-year period, signifying that every sample was incomplete. In Figure 3, from the first column to the fourth column (diversity ordered from high to low), the plots show the temporal diversity patterns for the asymptotic estimates, the standardized diversity under the incidence-based coverage value of C_{max} = 98.04%, observed diversity values, and the standardized diversity under the coverage value of C_{min} = 97.12% for 36 time periods. The plots in Figure 4 display the three dimensions of diversity in the same figure for each fixed order $q = 0$, 1 and 2.

4.1.3 | General patterns and conclusions (Figures 1–4)

Standardization is essential

As discussed above, regardless of data type (yearly abundance data or 3-year incidence data), sampling is incomplete and thus standardization to the same coverage is essential. Note that the observed yearly species richness pattern (Figure 1, row 1, column 3) reveals a gradual *increasing* tendency. However, when all samples are standardized to a fixed coverage, the trend becomes *decreasing* at the two standardized coverage values (row 1, columns 2 and 4 in both Figures 1 and 3); the decreasing trend is significant at the level of C_{min} = 97.12% (Figure 3, row 1, right panel). This reversal is mainly due to the relatively higher sample coverage values in most of the years after 2006. When diversity is standardized to a lower value of C_{min}, a majority of samples after 2006 are rarefied to lower diversities, leading to a declining trend.

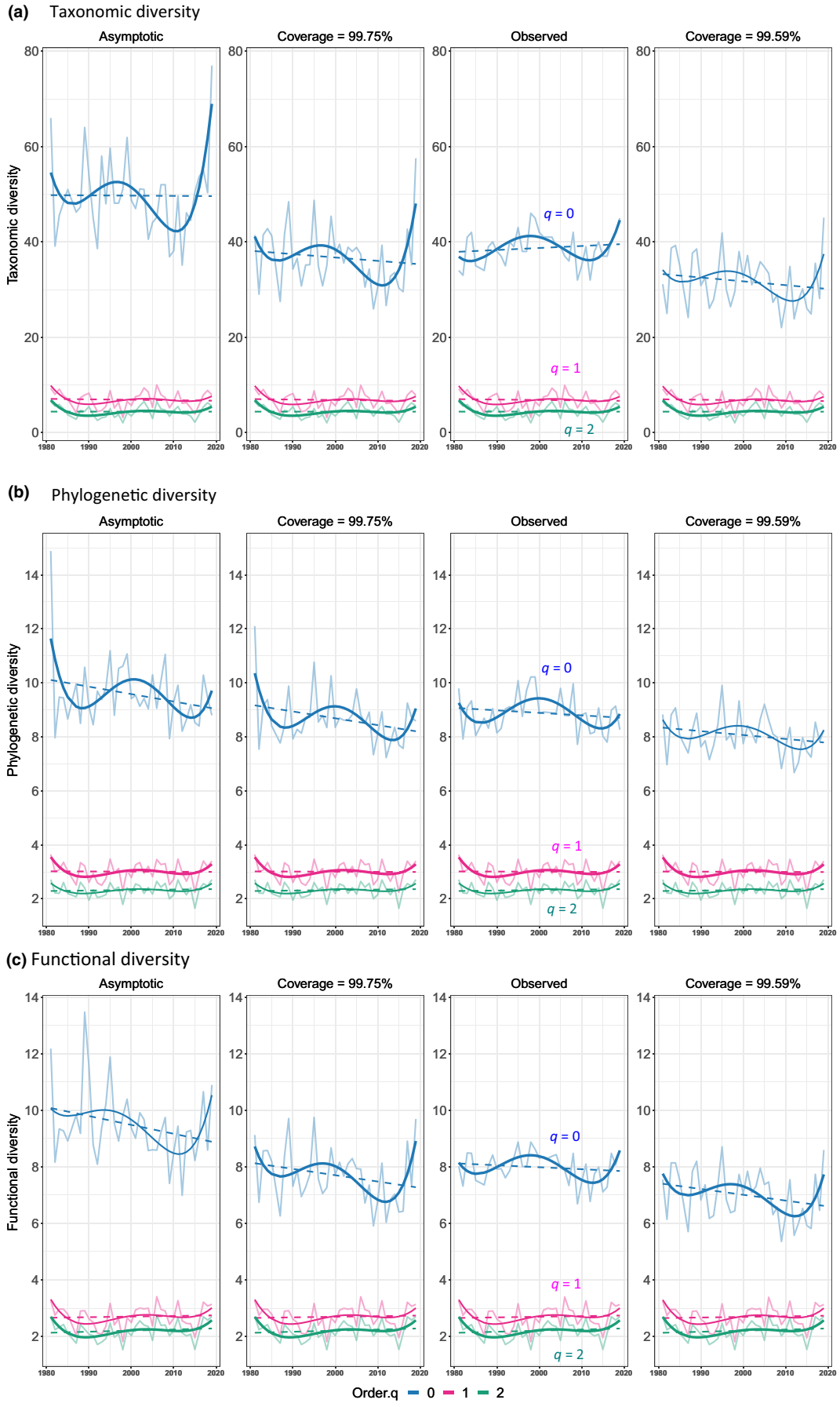

FIGURE 1 (Yearly abundance data). Temporal diversity patterns for TD (upper row), PD (middle row) and FD (the bottom row) based on yearly species fish abundance data (1981–2019, excluding 1986) for measures $q = 0$ (blue), $q = 1$ (pink) and $q = 2$ (green). The four columns (diversity values from high to low) represent, respectively, the curves for asymptotic estimates (column 1), standardized estimates under a coverage value of $C_{max} = 99.75\%$ (column 2), observed diversity (column 3), and standardized estimates under a coverage of $C_{min} = 99.59\%$ (column 4). All curves are fitted by a quartic polynomial and a linear trend. Statistical significance is denoted by a bold curve. Note the scale in *Y* axis is fixed in the same row, but the scale varies among different rows

A typical nonlinear *pattern for temporal diversity change*

All the diversity curves in Figures 1–4 can be fitted by quartic polynomials (a polynomial of degree 4), signifying general nonlinear biodiversity changes; most of the fits are significant. No matter whether the estimating target is on diversity changes over years (Figures 1 and 2) or over three consecutive years (Figures 3 and 4), the fitted nonlinear trends consistently suggest that each diversity initially declines in 1981, shortly increases up to a local maximum in 2000, then a decrease until 2010, and followed by a subsequent rise in recent years. To assess the long-term linear trend, we fit a linear regression to each curve in Figures 1–4; these linear trends are discussed below. We also fit all diversity series with more sophisticated GAMs (generalized additive models); the fitted smoothing curves exhibit similar patterns as the quartic polynomials. Therefore, we only focused on the simpler quartic polynomials.

The ordering among diversities

Figures 1 and 3 clearly show that for each dimension, the diversity decreases with the increasing order q, regardless of estimation method. Among TD, PD and FD measures, Figures 2 and 4 reveal that TD is always higher than the other two diversities. This reflects phylogenetic redundancy (because species are related based on their evolutionary histories) or functional redundancy (when certain species have similar traits and are functionally indistinct to some extent). There is no obvious ordering between PD and FD. For yearly abundance data, a general ordering TD > PD > FD is revealed among the three dimensions. For incidence data, TD remains the highest, but PD and FD exhibit a reversed ordering.

Patterns on TD, PD and FD diversity of q = *1 and* q = *2*

Due to the existence of some highly abundant species, the TD, PD and FD diversity values of $q = 1$ and $q = 2$ which incorporate species abundance are mainly influenced by these dominant species; nearly all these abundance-based diversity values are kept at a fixed value over 40 years, as also reflected by the nearly flat slopes in all fitted long-term linear trends. Note that for each fixed order ($q = 1$ or $q = 2$), the diversity values for the four estimation methods differ to a very limited extent. The undetected diversity (the difference between the asymptotic diversity and the observed diversity) can be accurately estimated by our methodology. Thus, for $q = 1$ and 2, the asymptotic estimates typically can be used to infer the true diversity.

Patterns on TD, PD and FD diversity of q = *0*

Unlike the measures of $q = 1$ and 2, the difference in diversity between the asymptotic estimate and the observed diversity for $q = 0$ are pronounced, signifying the undetected diversity can be substantial. Since our asymptotic estimates only represent lower bounds, fair comparisons of measures of $q = 0$ should be based on the two coverage-standardized diversity values. All the fitted linear trends for the two standardized coverages are slowly decreasing. Thus we can conclude that rare species (for TD), rare lineages (for PD) and rare functional groups (for FD) consistently decline over time at a very slow rate, whereas the above discussion for diversity of $q = 1$ and 2 implies that temporal diversity changes are limited for abundant and dominant ones.

4.2 | Effects of environmental drivers

We apply linear models to fit TD, PD and FD (specifically for diversity orders $q = 0$, 1 and 2) in terms of five environmental covariates: salinity (ppt), water temperature (degrees Celsius), North Atlantic Oscillation water Index (NAOI), sunspot number and river flow. We aim to build models that can explain the variance in the standardized diversity (as measured by the adjusted *R*-square) with the five independent environmental variables and their interactions. Under this goal, the variation involved in the monthly data and yearly data are too large to be fitted well. However, the environmental variables can be used to adequately explain the expected diversity computed from species 3-year incidence/occurrence data; the rarefied TD, PD and FD diversity estimates at the coverage value of $C_{min} = 97.12\%$ (right panels in Figures 3 and 4) are used as dependent variables for modeling purposes. We take the average of the monthly environmental data for every three consecutive years to form the independent variables in each time period. The pairwise correlation matrix and scatter plots of 14 variables including five environmental variables and nine standardized diversities (TD, PD and FD each with three diversity orders $q = 0$, 1 and 2) are shown in Figure S5.1.

In our model building, we first fitted a complicated model with all main effects and second-order (including two-variable interactions) effects. Then a stepwise model selection eliminated some variables that do not significantly contribute to the increase of the adjusted R^2 value. It turns out that river flow is not necessary, most likely due to its correlation with salinity and sunspot number. The models in Table S5.1 in Appendix S5 are our final choices for each dimension and each order; see Figure S5.2 for model fitting.

Our models suggest that *salinity*, *temperature and squared-temperature* are the most important variables for all three dimensions of biodiversity. These three variables are sufficient to explain >63% of the variation in the FD values. As for TD and PD, models depend on the focus and more variables are required. When the focus is on frequent and highly frequent species/lineages (TD and

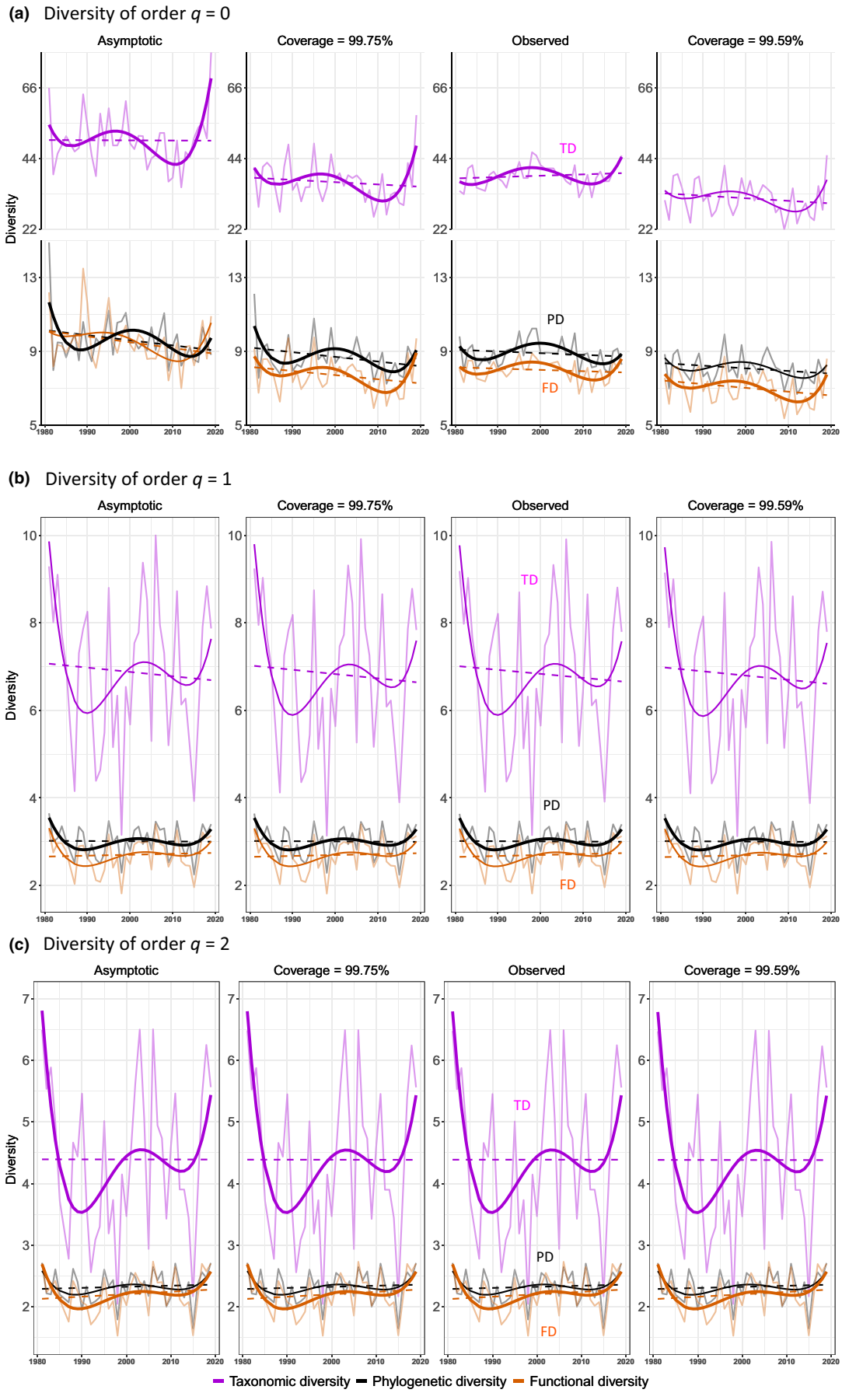

FIGURE 2 (Yearly abundance data with TD, PD and FD being plotted in the same figure for each order q). Temporal diversity patterns for the diversity of $q = 0$ (upper row), $q = 1$ (middle row) and $q = 2$ (lower row) based on yearly abundance data (1981–2019, excluding 1986) for TD (purple curves), PD (black curves) and FD (orange curves). The four columns represent, respectively, the diversity curves for asymptotic estimates (column 1), standardized estimates under a coverage value of $C_{max} = 99.75\%$ (column 2), observed diversity (column 3) and standardized estimates under a coverage of $C_{min} = 99.59\%$ (column 4). All curves are fitted by a quartic polynomial and a linear trend. Statistical significance is denoted by a bold curve. Note the scale in the *Y* axis is fixed in the same row, but the scale varies among different rows

PD of $q = 1$ and $q = 2$), adding the additional *sunspot* variable significantly improve the fitting. When the focus is on rare species/lineages (i.e. TD and PD of order $q = 0$) which vary with more covariates, four additional variables (NAOI, sunspot, squared sunspot and the interaction of NAOI and sunspot) should be included in the model.

All selected models reveal that diversity declines when salinity is increased. The magnitude of decline diminishes with increasing order q: For TD of $q = 0$, 1 and 2, the effects are 3.32, 1.27 and 0.94. The corresponding effects are 0.68, 0.51 and 0.45 for FD, and 0.43, 0.17 and 0.15 for PD. The effect of temperature on diversity is generally *quadratic*, not linear. The quadratic temperature effect implies that all else being equal, fish diversity attains the highest value around 13–14 degrees (Celsius). The two exceptions are PD of $q = 1$ and $q = 2$ for which temperature effect is linear. Note that the PD values of these two orders are dominated by the abundant/frequent nodes in the phylogenetic tree and thus are mainly determined by the deep nodes (i.e. ancient ancestors). These deep nodes are less sensitive to temperature changes and exhibit an increasing linear trend with temperature. The effects of the other two environment variables (sunspot and NAOI) are assessed in Appendix S5. All effects can be meaningfully interpreted; see Discussion below.

5 | DISCUSSION

The patterns shown in Figures 1–4 extend existing insights into biodiversity change in the Bridgwater Bay fish assemblage in key ways. This is a system that is broadly stable, over time, in terms of the abundances of its core taxa (Henderson & Magurran, 2014). However, as our new analysis makes clear, this 'headline' stability is underlain by nonlinear patterns of change in the three dimensions of diversity. The models described in Section 4.2 reveal that these trends have an ecological interpretation. For instance, a high proportion of the variability in FD (>60%) relates to changes in salinity and temperature, with greatest FD at intermediate average temperatures. Bridgwater Bay is a lower estuary with salinity typically ranging from 22% to 32%. Reduced salinity reflects greater river flow and increased allochthonous inputs leading to increased productivity. During periods of lower salinity (high flow) prey species, such as brown shrimp *Crangon crangon* move into the Bay from upper estuarine locations (Henderson et al., 2006) generating a burst in productivity and FD as the food base expands. Similarly, maximum FD at intermediate temperatures can be related to trophic ecology. At low temperatures fish move towards warmer and often deeper oceanic waters reducing FD. Conversely, in summer, when local water temperatures can exceed 22°C there is a retreat into deeper, cooler, oxygen richer waters resulting in a seasonal minimum in fish diversity which is most marked in the warmest years.

A further example relates to the TD and PD models that required the addition of the NAOI and sunspot variables to get an adequate fit. These variables are linked to large-scale oceanic features which determine both the dynamics and growth of abundant species and the arrival of rare forms. The NAOI is a summarizing variable for a suite of climatic factors including rainfall, river flow, salinity, temperature and wind direction and its magnitude is linked to the position of the gulf stream. It is known to have a major influence on the dominant fish within Bridgwater Bay. For instance, the NAOI is positively correlated with sprat *Sprattus sprattus* recruitment (Henderson & Henderson, 2017) and whiting *Merlangius merlangus* growth (Henderson, 2019).

Like many other ecological assemblages, this is a system in which most of the biomass is provided by a handful of persistent (core) species, and most of the richness by many rare taxa, which are often transient (Henderson & Magurran, 2014; Magurran & Henderson, 2003). Hill-Chao numbers shed light on different contributions of the abundant/rare (persistent/transient) taxa to biodiversity change at Bridgwater Bay for each of the dimensions of diversity (Figures 1–4). This informs a mechanistic understanding of baseline change in ecological assemblages (Dornelas et al., 2013). As illustrated by our analysis of the four-decade estuarine assemblage, iNEXT.3D has considerable potential in interpretating and predicting the restructuring of ecological communities in response to climate change and other anthropogenic stressors.

6 | CONCLUSIONS

In this paper, the three dimensions (TD, PD and FD) of biodiversity are integrated under a common framework referred to as the attribute diversity or Hill-Chao numbers; see Equation (2). The theoretical framework is summarized in Table 1. At the sampling data level, when data do not contain sufficient information to infer the true diversity (especially TD, PD and FD diversities of $q = 0$), the proposed iNEXT.3D standardization (in Section 3) via coverage-based rarefaction and extrapolation is recommended to make fair comparison of diversity over time; see Section 4 for an example and Figures 1–4 for temporal diversity change patterns.

Although we have applied the iNEXT.3D standardization to temporal data, the method can be applied to spatial data to measure diversity change across space or along an environmental gradient. The

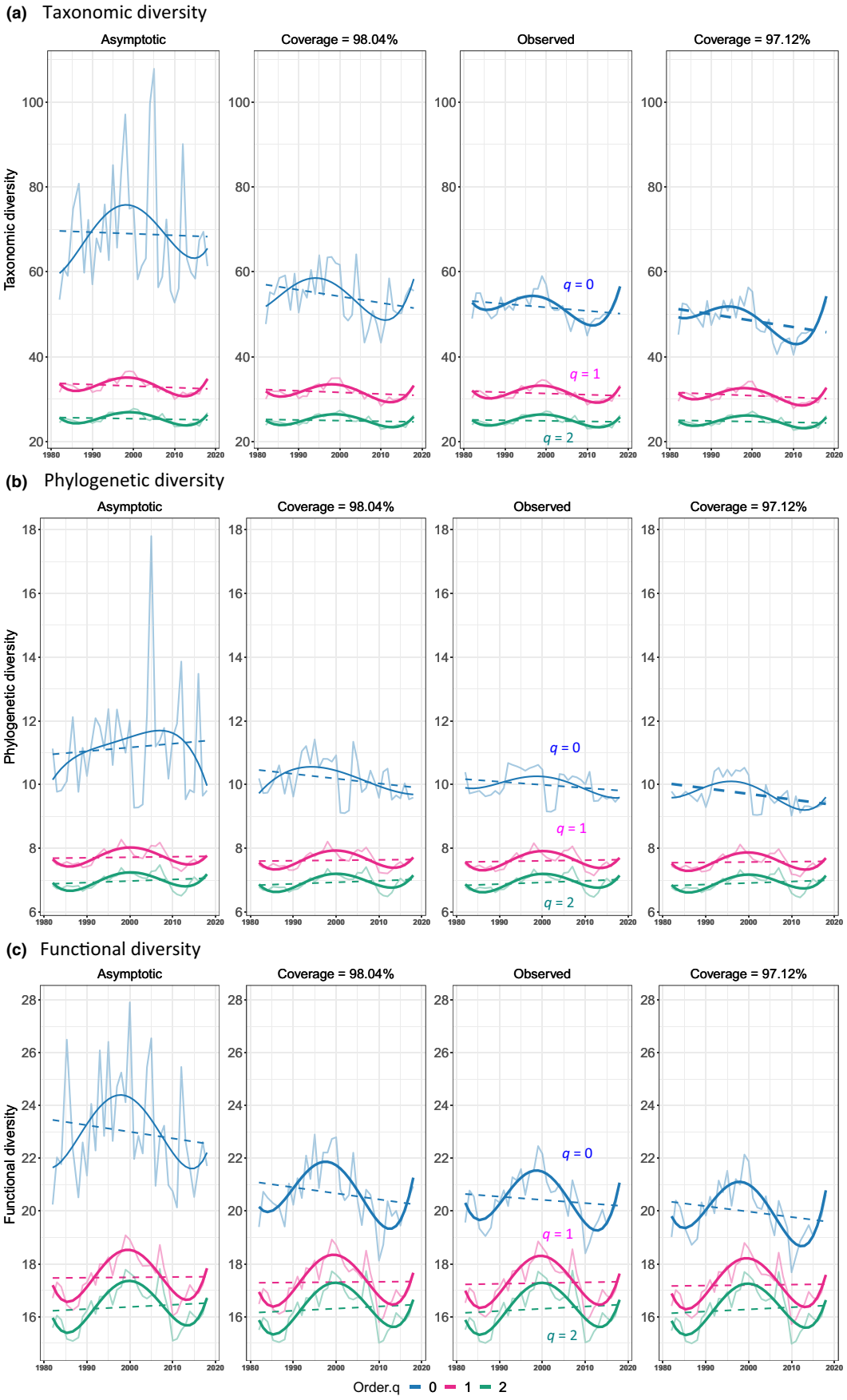

FIGURE 3 (Three-year incidence data) See the legend of Figure 1, but with the following changes: C_{max} = 98.04% and C_{min} = 97.12% based on monthly incidence data for three consecutive years

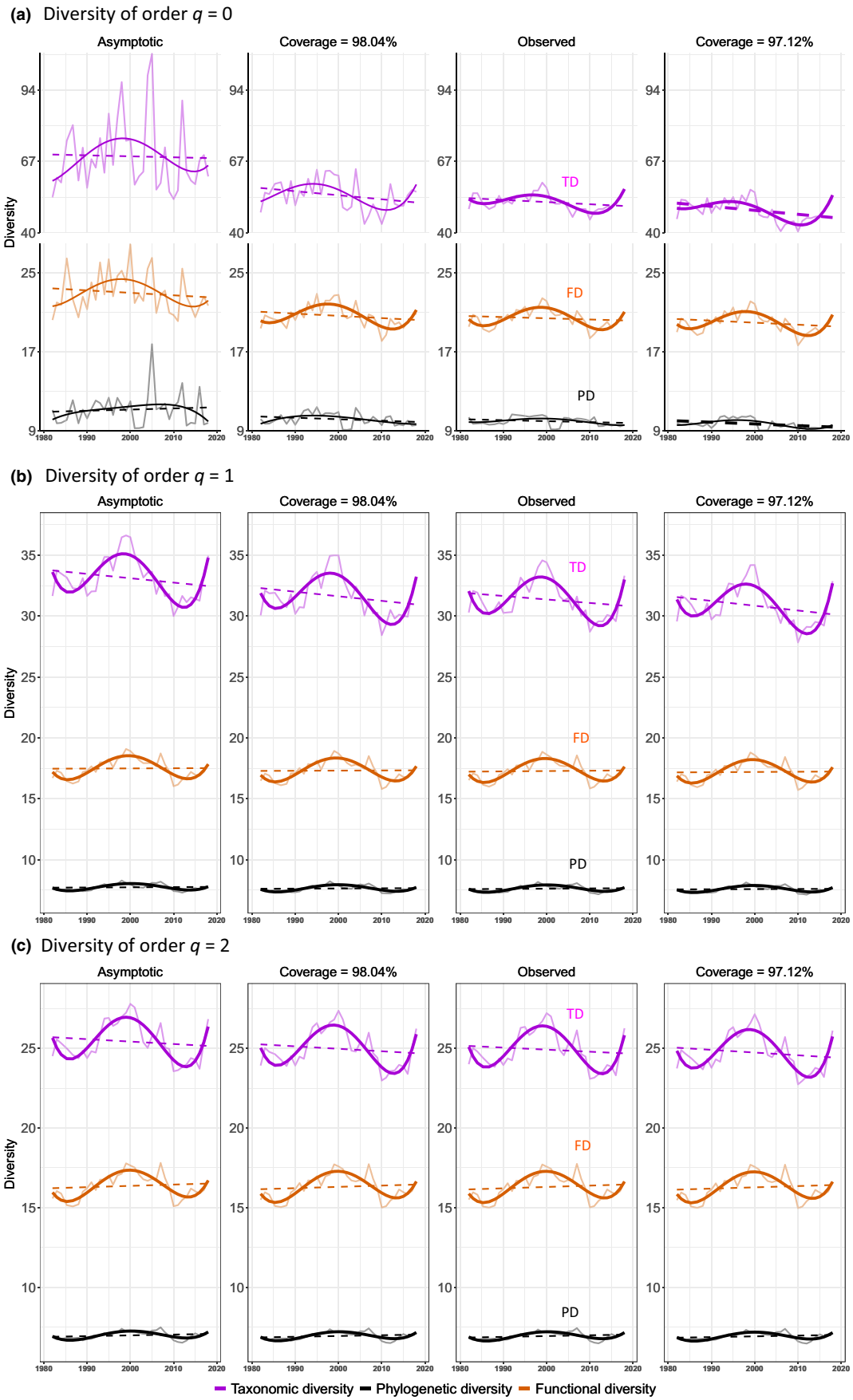

FIGURE 4 (Three-year incidence data with TD, PD and FD being plotted in the same figure for each order q). See the legend of Figure 2, but with the following changes: C_{max} = 98.04% and C_{min} = 97.12% based on monthly incidence data for three consecutive years

extension of the iNEXT standardization to beta diversity is under development and will be reported in later stages.

ACKNOWLEDGEMENTS

We are grateful to an Associate Editor (Will Pearse) and three reviewers for the very thoughtful and insightful comments and suggestions. This work is jointly supported by the Natural Environment Research Council, UK (NE/T004487/1 for A.E.M. and M.D.) and the Taiwan Ministry of Science and Technology under Contracts NERC-MOST 108-2923-M-007-003 (for A.C. and C.-H.C.). A.E.M. and M.D. also acknowledge support from the Leverhulme Trust (RPG-2019-402). We thank Ada Fontrodona Eslava for comments on the paper.

CONFLICT OF INTEREST

The authors declare no conflict of interest.

AUTHORS' CONTRIBUTIONS

A.C., C.-H.C., M.D. and A.E.M. conceived the ideas; P.A.H. collected the taxonomic data and environmental variables; F.M. constructed the phylogenetic tree and collected all traits data. C.-H.C. and K.--H.H. developed the software and graphics; A.C. and C.-H.C. analysed the data and all authors contributed to the interpretation of the results. A.C. and A.E.M. led the writing, and all authors edited the manuscript.

PEER REVIEW

The peer review history for this article is available at https://publons.com/publon/10.1111/2041-210X.13682.

DATA AVAILABILITY STATEMENT

All R codes along with data used in this paper are archived in Zenodo repository https://doi.org/10.5281/zenodo.4992797 (Chao, 2021; Chao et al., 2021). Data are also available at University of St Andrews https://doi.org/10.17630/648b0d8c-aacd-4416-9844-833e6436f71a. For readers without R background, the online software 'iNEXT.3D' is available from https://chao.shinyapps.io/iNEXT.3D/ to facilitate all computation and graphics.

ORCID

Anne Chao https://orcid.org/0000-0002-4364-8101
Peter A. Henderson https://orcid.org/0000-0002-7461-1758
Chun-Huo Chiu https://orcid.org/0000-0002-7096-2278
Faye Moyes https://orcid.org/0000-0001-9687-0593
Maria Dornelas https://orcid.org/0000-0003-2077-7055
Anne E. Magurran https://orcid.org/0000-0002-0036-2795

REFERENCES

Arnan, X., Cerdá, X., & Retana, J. (2017). Relationships among taxonomic, functional, and phylogenetic ant diversity across the biogeographic regions of Europe. *Ecography*, *40*, 448–457. https://doi.org/10.1111/ecog.01938

Bjorkman, A. D., Myers-Smith, I. H., Elmendorf, S. C., Normand, S., Rüger, N., Beck, P. S. A., Blach-Overgaard, A., Blok, D., Cornelissen, J. H. C., Forbes, B. C., Georges, D., Goetz, S. J., Guay, K. C., Henry, G. H. R., HilleRisLambers, J., Hollister, R. D., Karger, D. N., Kattge, J., Manning, P., … Weiher, E. (2018). Plant functional trait change across a warming tundra biome. *Nature*, *562*, 57–62. https://doi.org/10.1038/s41586-018-0563-7

Cadotte, M. W., Carscadden, K., & Mirotchnick, N. (2011). Beyond species: Functional diversity and the maintenance of ecological processes and services. *Journal of Applied Ecology*, *48*, 1079–1087. https://doi.org/10.1111/j.1365-2664.2011.02048.x

Cadotte, M. W., & Davies, T. J. (2016). *Phylogenies in ecology: A guide to concepts and methods*. Princeton University Press.

Chao, A. (2021). MEE_iNEXT.3D (R code and data for graphics in MEE 2021 paper by Chao et al.). University of St Andrews, https://doi.org/10.17630/648b0d8c-aacd-4416-9844-833e6436f71a

Chao, A., Chiu, C.-H., & Jost, L. (2010). Phylogenetic diversity measures based on Hill numbers. *Philosophical Transactions of the Royal Society B: Biological Sciences*, *365*, 3599–3609. https://doi.org/10.1098/rstb.2010.0272

Chao, A., Chiu, C.-H., Villéger, S., Sun, I.-F., Thorn, S., Lin, Y.-C., Chiang, J.-M., & Sherwin, W. B. (2019). An attribute-diversity approach to functional diversity, functional beta diversity, and related (dis)similarity measures. *Ecological Monographs*, *89*, e01343. https://doi.org/10.1002/ecm.1343

Chao, A., Gotelli, N. G., Hsieh, T. C., Sander, E. L., Ma, K. H., Colwell, R. K., & Ellison, A. M. (2014). Rarefaction and extrapolation with Hill numbers: A framework for sampling and estimation in species biodiversity studies. *Ecological Monographs*, *84*, 45–67.

Chao, A., Henderson, P. A., Chiu, C.-H., Moyes, F., Hu, K.-H., Dornelas, M., & Magurran, A. E. (2021). Data from: Measuring temporal change in alpha diversity: a framework integrating taxonomic, phylogenetic and functional diversity and the iNEXT.3D standardization. *Zenodo*, https://doi.org/10.5281/zenodo.4992797

Chao, A., & Jost, L. (2012). Coverage-based rarefaction: Standardizing samples by completeness rather than by size. *Ecology*, *93*, 2533–2547.

Chao, A., Kubota, Y., Zelený, D., Chiu, C.-H., Li, C.-F., Kusumoto, B., Yasuhara, M., Thorn, S., Wei, C.-L., Costello, M. J., & Colwell, R. K. (2020). Quantifying sample completeness of a biological survey and comparing diversities among assemblages based on incomplete surveys. *Ecological Research*, *35*, 292–314.

Chase, J. M., Blowes, S. A., Knight, T. M., Gerstner, K., & May, F. (2020). Ecosystem decay exacerbates biodiversity loss with habitat loss. *Nature*, *584*, 238–243. https://doi.org/10.1038/s41586-020-2531-2

Chun, J.-H., & Lee, C.-B. (2017). Disentangling the local-scale drivers of taxonomic, phylogenetic and functional diversity in woody plant assemblages along elevational gradients in South Korea. *PLoS ONE*, *12*, e0185763. https://doi.org/10.1371/journal.pone.0185763

Colwell, R. K., Chao, A., Gotelli, N. J., Lin, S. Y., Mao, C. X., Chazdon, R. L., & Longino, J. T. (2012). Models and estimators linking individual-based and sample-based rarefaction, extrapolation, and comparison of assemblages. *Journal of Plant Ecology*, *5*, 3–21. https://doi.org/10.1093/jpe/rtr044

Daskalova, G. N., Myers-Smith, I. H., Bjorkman, A. D., Blowes, S. A., Supp, S. R., Magurran, A. E., & Dornelas, M. (2020). Landscape-scale forest loss as a catalyst of population and biodiversity change. *Science*, *368*, 1341–1347. https://doi.org/10.1126/science.aba1289

Diaz, S., & Cabido, M. (1997). Plant functional types and ecosystem function in relation to global change. *Journal of Vegetation Science*, *8*, 463–474. https://doi.org/10.1111/j.1654-1103.1997.tb00842.x

Díaz, S., Demissew, S., Carabias, J., Joly, C., Lonsdale, M., Ash, N., Larigauderie, A., Adhikari, J. R., Arico, S., Báldi, A., Bartuska, A., Baste, I. A., Bilgin, A., Brondizio, E., Chan, K. M. A., Figueroa, V. E., Duraiappah, A., Fischer, M., Hill, R., … Zlatanova, D. (2015). The IPBES conceptual framework – Connecting nature and people. *Current Opinion in Environmental Sustainability*, *14*, 1–16. https://doi.org/10.1016/j.cosust.2014.11.002

Dornelas, M., Gotelli, N. J., McGill, B., Shimadzu, H., Moyes, F., Sievers, C., & Magurran, A. E. (2014). Assemblage time series reveal biodiversity

change but not systematic loss. *Science*, *344*, 296–299. https://doi.org/10.1126/science.1248484

Dornelas, M., Magurran, A. E., Buckland, S. T., Chao, A., Chazdon, R. L., Colwell, R. K., Curtis, T., Gaston, K. J., Gotelli, N. J., Kosnik, M. A., McGill, B., McCune, J. L., Morlon, H., Mumby, P. J., Øvreås, L., Studeny, A., & Vellend, M. (2013). Quantifying temporal change in biodiversity: Challenges and opportunities. *Proceedings of the Royal Society B: Biological Sciences*, *280*, 20121931. https://doi.org/10.1098/rspb.2012.1931

Faith, D. P. (1992). Conservation evaluation and phylogenetic diversity. *Biological Conservation*, *61*, 1–10. https://doi.org/10.1016/0006-3207(92)91201-3

Frishkoff, L. O., Karp, D. S., M'Gonigle, L. K., Mendenhall, C. D., Zook, J., Kremen, C., Hadly, E. A., & Daily, G. C. (2014). Loss of avian phylogenetic diversity in neotropical agricultural systems. *Science*, *345*, 1343–1346. https://doi.org/10.1126/science.1254610

Good, I. J. (1953). The population frequencies of species and the estimation of population parameters. *Biometrika*, *40*, 237–264. https://doi.org/10.1093/biomet/40.3-4.237

Gower, J. C. (1971). A general coefficient of similarity and some of its properties. *Biometrics*, *27*, 857–871. https://doi.org/10.2307/2528823

Helmus, M. R., Mahler, D. L., & Losos, J. B. (2014). Island biogeography of the Anthropocene. *Nature*, *513*, 543–546.

Henderson, P. A. (2019). A long-term study of whiting, *Merlangius merlangus* (L) recruitment and population regulation in the Severn Estuary, UK. *Journal of Sea Research*, *155*, 101825. https://doi.org/10.1016/j.seares.2019.101825

Henderson, P. A., & Henderson, R. C. (2017). Population regulation in a changing environment: Long-term changes in growth, condition and survival of sprat, *Sprattus sprattus* L. in the Bristol Channel, UK. *Journal of Sea Research*, *120*, 24–34. https://doi.org/10.1016/j.seares.2016.11.003

Henderson, P. A., & Holmes, R. H. A. (1991). On the population dynamics of dab, sole and flounder within Bridgwater bay in the lower severn estuary, England. *Netherlands Journal of Sea Research*, *27*, 337–344. https://doi.org/10.1016/0077-7579(91)90036-Z

Henderson, P. A., & Magurran, A. E. (2014). Direct evidence that density-dependent regulation underpins the temporal stability of abundant species in a diverse animal community. *Proceedings of the Royal Society B: Biological Sciences*, *281*, 20141336. https://doi.org/10.1098/rspb.2014.1336

Henderson, P. A., Seaby, R. M., & Somes, J. R. (2006). A 25-year study of climatic and density-dependent population regulation of common shrimp *Crangon crangon* (Crustacea: Caridea) in the Bristol Channel. *Journal of the Marine Biological Association of the United Kingdom*, *86*, 287–298.

Henderson, P. A., Seaby, R. M., & Somes, J. R. (2011). Community level response to climate change: The long-term study of the fish and crustacean community of the Bristol Channel. *Journal of Experimental Marine Biology and Ecology*, *400*, 78–89. https://doi.org/10.1016/j.jembe.2011.02.028

Hill, M. O. (1973). Diversity and evenness: A unifying notation and its consequences. *Ecology*, *54*, 427–432. https://doi.org/10.2307/1934352

Hsieh, T. C., & Chao, A. (2017). Rarefaction and extrapolation: Making fair comparison of abundance-sensitive phylogenetic diversity among multiple assemblages. *Systematic Biology*, *66*, 100–111.

Hsieh, T.-C., Ma, K. H., & Chao, A. (2016). iNEXT: An R package for rarefaction and extrapolation of species diversity (Hill numbers). *Methods in Ecology and Evolution*, *7*, 1451–1456.

Magurran, A. E., & Henderson, P. A. (2003). Explaining the excess of rare species in natural species abundance distributions. *Nature*, *422*, 714–716. https://doi.org/10.1038/nature01547

Magurran, A. E., & McGill, B. J. (Eds.). (2011). *Biological diversity: Frontiers in measurement and assessment*. Oxford University Press.

Maire, E., Grenouillet, G., Brosse, S., & Villéger, S. (2015). How many dimensions are needed to accurately assess functional diversity? A pragmatic approach for assessing the quality of functional spaces. *Global Ecology and Biogeography*, *24*, 728–740. https://doi.org/10.1111/geb.12299

Petchey, O. L., & Gaston, K. J. (2002). Functional diversity (FD), species richness and community composition. *Ecology Letters*, *5*, 402–411. https://doi.org/10.1046/j.1461-0248.2002.00339.x

Pillar, V. D., & Duarte, L. S. (2010). A framework for metacommunity analysis of phylogenetic structure. *Ecology Letters*, *13*, 587–596. https://doi.org/10.1111/j.1461-0248.2010.01456.x

Rao, C. R. (1982). Diversity and dissimilarity coefficients: A unified approach. *Theoretical Population Biology*, *21*, 24–43. https://doi.org/10.1016/0040-5809(82)90004-1

Southwood, T. R. E., & Henderson, P. A. (2000). *Ecological methods* (3rd ed.). Blackwell Science.

Swenson, N. G. (2019). *Phylogenetic ecology: A history, critique, and remodeling*. The University of Chicago Press.

Tilman, D., Knops, J., Wedin, D., Reich, P. B., Ritchie, M., & Siemann, E. (1997). The influence of functional diversity and composition on ecosystem processes. *Science*, *277*, 1300–1302. https://doi.org/10.1126/science.277.5330.1300

Tucker, C. M., Cadotte, M. W., Carvalho, S. B., Davies, T. J., Ferrier, S., Fritz, S. A., Grenyer, R., Helmus, M. R., Jin, L. S., Mooers, A. O., Pavoine, S., Purschke, O., Redding, D. W., Rosauer, D. F., Winter, M., & Mazel, F. (2017). A guide to phylogenetic metrics for conservation, community ecology and macroecology. *Biological Reviews*, *92*, 698–715. https://doi.org/10.1111/brv.12252

Villéger, S., Brosse, S., Mouchet, M., Mouillot, D., & Vanni, M. J. (2017). Functional ecology of fish: Current approaches and future challenges. *Aquatic Sciences*, *79*, 783–801. https://doi.org/10.1007/s00027-017-0546-z

SUPPORTING INFORMATION

Additional supporting information may be found online in the Supporting Information section.

How to cite this article: Chao, A., Henderson, P. A., Chiu, C.-H., Moyes, F., Hu, K.-H., Dornelas, M., & Magurran, A. E. (2021). Measuring temporal change in alpha diversity: A framework integrating taxonomic, phylogenetic and functional diversity and the iNEXT.3D standardization. *Methods in Ecology and Evolution*, 12, 1926–1940. https://doi.org/10.1111/2041-210X.13682